Physics of Plasmas

Self-organized magnetic equilibria in tokamak plasmas with very low edge safety factor

Cite as: Phys. Plasmas **29**, 080704 (2022); https://doi.org/10.1063/5.0101880
Submitted: 03 June 2022 • Accepted: 25 July 2022 • Published Online: 19 August 2022

N. C. Hurst, B. E. Chapman, A. F. Almagri, et al.

COLLECTIONS

This paper was selected as an Editor's Pick

Physics of Plasmas LETTER scitation.org/journal/php

Self-organized magnetic equilibria in tokamak plasmas with very low edge safety factor

Cite as: Phys. Plasmas **29**, 080704 (2022); doi: 10.1063/5.0101880
Submitted: 3 June 2022 · Accepted: 25 July 2022 ·
Published Online: 19 August 2022

N. C. Hurst,[1,a] B. E. Chapman,[1] A. F. Almagri,[1] B. S. Cornille,[2] S. Z. Kubala,[1] K. J. McCollam,[1] J. S. Sarff,[1] C. R. Sovinec,[2] J. K. Anderson,[1] D. J. Den Hartog,[1] C. B. Forest,[1] M. D. Pandya,[1] and W. S. Solsrud[1]

AFFILIATIONS

[1]Department of Physics, University of Wisconsin-Madison, Madison, Wisconsin 53706, USA
[2]Department of Engineering Physics, University of Wisconsin-Madison, Madison, Wisconsin 53706, USA

[a]Author to whom correspondence should be addressed: nhurst@wisc.edu

ABSTRACT

Tokamak plasmas often exhibit self-organizing behavior in which internal modes shape the toroidal current density profile, a common example being the sawtooth instability. However, such behavior has not been studied in detail for edge safety factor below 2 due to disruptive kink instabilities that typically prevent operation in this regime. Now, steady tokamak plasmas with an edge safety factor down to 0.8 have been created in the Madison Symmetric Torus, where disruptions are prevented due to a thick, conductive wall and a feedback power supply that sustains the plasma current. Internal measurements and nonlinear magnetohydrodynamic modeling reveal a family of safety factor profiles with a central value clamped near unity as the edge safety factor decreases, indicating current profile broadening through a relaxation process. As the safety factor decreases, the magnetic fluctuations become irregular, and the electron energy confinement time decreases.

The radial distribution of current flowing inside tokamak plasmas is often shaped through a self-organization process[1] where internal, helical kink modes influence their own stability by driving transport. A classic example is the sawtooth instability, which regulates peaking of the current density profile in most tokamaks and remains a topic of active research.[2–6] This process is thought to impose a lower bound on the central safety factor, $q(0) \approx 1$, where $q(r)$ is the ratio of toroidal to poloidal winding number for the equilibrium magnetic field, and r is the minor radius. A lower bound is also routinely observed for the edge safety factor, $q(a) \propto B_\phi/I_p \geq 2$, where a is the plasma minor radius, B_ϕ is the toroidal field, and I_p is the plasma current, below which the growth of external kink modes disrupts the discharge.[4,7,8] This has prevented detailed studies of current profile relaxation and central safety factor behavior in the regime $q(a) < 2$. Furthermore, the limitation on I_p for a given applied B_ϕ is detrimental to the goal of sustained nuclear fusion, since energy confinement, Ohmic heating, and the empirical Greenwald density limit scale with I_p.[9,10] If the disruption can be avoided, a relatively unexplored, high-current regime can be accessed and studied in which strong self-organization and magnetohydrodynamic (MHD) kink dynamics are expected. Similar kink-mediated relaxation is commonly observed in reversed-field pinch (RFP) and spheromak plasmas,[11–13] Z-pinches,[14,15] solar flares,[16–18] cylindrical plasma flux-rope experiments,[19–21] and twisted vortex lines in neutral fluids.[22]

Kink instabilities in toroidal plasmas are resonant on rational magnetic surfaces with $q = m/n$, where m and n are the poloidal and toroidal mode numbers. In the presence of a metallic boundary, the external kink at the plasma edge becomes a resistive wall mode (RWM) which grows on the characteristic wall time, τ_w, for resistive diffusion of magnetic field into the boundary.[23,24] Progress has been made to circumvent the disruptive instability at $q(a) = 2$ by using active magnetic feedback to stabilize the RWM for tokamak plasmas in the DIII-D ($\tau_w = 2.5$ ms) and RFX-mod ($\tau_w = 50$ ms) devices.[25,26] DIII-D obtained edge safety factor 1.87 by transiently ramping the plasma current upward. RFX-mod obtained $q(a) = 1.55$ in steady conditions, but the internal magnetic equilibrium and confinement were not measured. Uncontrolled, transient, tokamak-like discharges have been studied in a few cases for $q(a) < 1$[27–30] and for $1 < q(a) < 2$[31–35] due to their role in RFP startup physics and interest in high-current tokamak operation, but detailed analysis of equilibria and fluctuations was difficult in these short discharges of duration ~5 ms. Recently, longer discharges (~100 ms) with $q(a) < 1$ have been studied in RFX-mod, with a focus on MHD activity during stepwise evolution of the plasma current.[36] The $q(a) = 2$ threshold has also

been crossed in stellarator–tokamak hybrid discharges where a fraction of the rotational transform is supplied externally.[37] Nonlinear MHD simulations have been conducted in a few cases for $q(a) < 1$,[36,38–40] but otherwise the $q(a) < 2$ regime has received little attention from modern numerical simulations and theoretical analysis. Thus, although the tokamak is the most widely studied magnetic fusion concept, the $q(a) < 2$ regime is neither well characterized nor well understood.

In this Letter, we report on the equilibrium, fluctuation, and confinement properties of steady, well-controlled tokamak plasmas with very low edge safety factor $0.8 \leq q(a) \leq 3$, with a focus on the range $1 < q(a) < 2$. Measurements were made in the Madison Symmetric Torus (MST) device,[41] where the disruptive RWM instability is mitigated passively due to a thick, close-fitting shell with $\tau_w \approx 800$ ms, and $q(a)$ is held constant by feedback-controlled programmable power supplies (PPS) driving both B_ϕ and I_p.[42,43] This permits the study of internally resonant tearing modes and transport physics for $q(a) < 2$ without the complicating factors of external modes or inductive effects. A deep-insertion magnetic probe reveals a family of $q(r)$ profiles that appear to be clamped near unity in the core, with a flat region that expands outward as $q(a)$ decreases toward 1, reflecting a self-organized flattening of the toroidal current density profile. Magnetic fluctuation behavior changes from periodic sawtooth crashes to irregular, quasi-continuous relaxation as $q(a)$ decreases. The electron energy confinement time decreases for $q(a) < 2$. Numerical simulations using the nonlinear MHD code NIMROD,[44] initiated with low-$q(a)$ experimental equilibria and Lundquist number $S \sim 10^5$, also exhibit $q(r)$ profiles which relax toward unity in the core.

The MST is a toroidal plasma device with major radius $R = 1.5$ m and minor radius 0.52 m, where fixed graphite limiters restrict the plasma radius to $a = 0.5$ m.[41] It was primarily designed and used to study RFP physics[45] but has recently been operated as a low-current tokamak.[46] It features a 5 cm thick aluminum vacuum vessel with a circular poloidal cross section which also serves as a close-fitting conducting shell and a single-turn toroidal field winding. The PPS systems use pulse width modulation with feedback control to meet arbitrary user-specified demand waveforms.[42,43] In all plasmas described here, a flat $B_\phi = 0.133$ T waveform is produced with duration 40 ms $\ll \tau_w$. Thus, during the discharges, surface-normal magnetic perturbations are inhibited, and external modes are passively stabilized due to eddy current flowing in the shell.

The toroidal plasma current was varied from 40 to 165 kA with flat-topped waveforms, such that $q(a)$ was held constant in the range 0.8–3. Any value of $q(a)$ in this range is attainable. The measured cylindrical safety factor, $q_c(a) = 2\pi a^2 \langle B_\phi(a) \rangle / \mu_0 R I_p$, is shown in Fig. 1(a), where $\langle \cdot \rangle$ indicates a flux surface average, and μ_0 is the permeability of free space. The cylindrical approximation to q is about 10% lower at the plasma edge than that obtained from toroidal equilibrium reconstructions, where the latter is important to understand MHD kink stability, but the former is more easily measured. The surface toroidal voltage, $V_\phi(a)$, equal to the resistive loop voltage in steady-state, is shown in Fig. 1(b) with a running 0.3 ms time average. For $q_c(a) = 2.7$ (black waveforms), $V_\phi(a)$ varies periodically with the sawtooth cycle at a frequency of about 0.4 kHz. The variations in $V_\phi(a)$ are due to the PPS feedback circuit reacting to internal magnetic relaxation as well as changes in plasma resistivity. As $q(a)$ decreases toward 1, increased frequency and irregularity are observed.

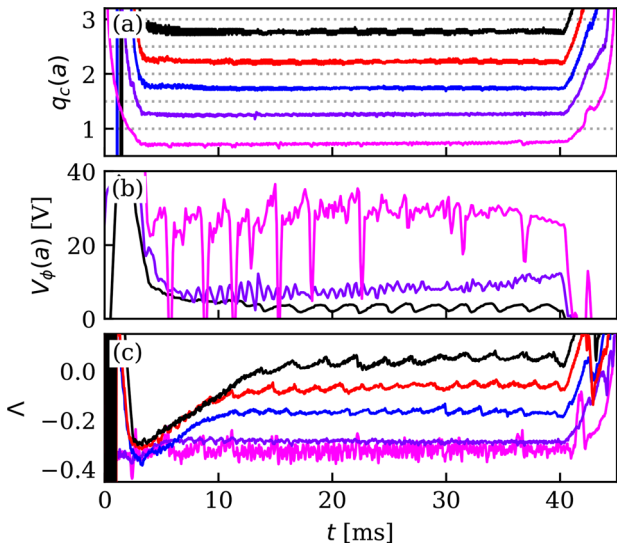

FIG. 1. Waveforms of (a) cylindrical edge safety factor, (b) surface toroidal voltage, and (c) poloidal asymmetry factor for discharges with $0.7 \leq q_c(a) \leq 2.7$ (data for a given discharge denoted by the same color in all panels). Data for $q_c(a) = 2.2$ and 1.7 are omitted in panel (b) for clarity since V_ϕ is similar to that of $q_c(a) = 2.7$.

The loop voltage increases from 2–3 V up to ∼30 V in the range $2.7 \geq q_c(a) \geq 0.7$. For $q_c(a) = 0.7$ (magenta waveforms), the voltage swings dramatically due to strong kink activity. For all data shown here, the working gas was deuterium, and the line-averaged electron density was in the range $0.35–0.55 \times 10^{19}$ m^{-3}, where the upper bound is near the Greenwald limit[10] for $q(a) = 3$.

Internal properties of tokamak plasmas can be inferred using edge measurements of the poloidal field asymmetry factor $\Lambda = \tilde{b}_{\theta 1}(a) R / a B_\theta = l_i/2 + \beta_p - 1$, where $\tilde{b}_{\theta 1}(a)$ is the $m = 1$, $n = 0$ spatial Fourier component of the poloidal field measured by coil arrays mounted on the inner surface of the conducting wall, $l_i = \langle B_\theta^2 \rangle / B_\theta^2(a)$ is the volume-averaged internal inductance, and $\beta_p \equiv 2\mu_0 \langle p \rangle / B_\theta^2(a)$ is the plasma pressure normalized to the edge poloidal field pressure.[47] Waveforms of Λ are shown in Fig. 1(c). Thermal pressure is relatively small in these Ohmically heated plasmas, so Λ is dominated by l_i, which increases with peaking of the toroidal current density profile, $j_\phi(r)$. Thus, early upward evolution of Λ is associated with diffusive current peaking, which halts due to the $m/n = 1/1$ sawtooth instability when the core safety factor, $q(0)$, drops below unity. Lower-$q(a)$ discharges reach steady-state earlier, since less current peaking is required to reach $q(0) = 1$. Lower $q(a)$ results in broader $j_\phi(r)$ and, therefore, flatter $q(r)$ profiles.

Internal diagnosis is accomplished using Thomson scattering, which measures the electron temperature, T_e, at 21 radial locations $r/a \leq 0.8$;[48] interferometry, which measures the electron density, n_e, along 11 vertical chords spanning the plasma diameter;[49] and a deep-insertion magnetic probe, which provides local field measurements in all three directions at 20 radial locations, $r/a \geq 0.69$. All of these data constrain toroidal equilibrium reconstructions using the MSTFit code.[50]

Figure 2(a) shows $q_c(r)$ profiles obtained from probe data averaged over $27.5 \leq t \leq 32.5$ ms, after all discharges have reached steady-state. The data reveal a family of profiles which approach unity

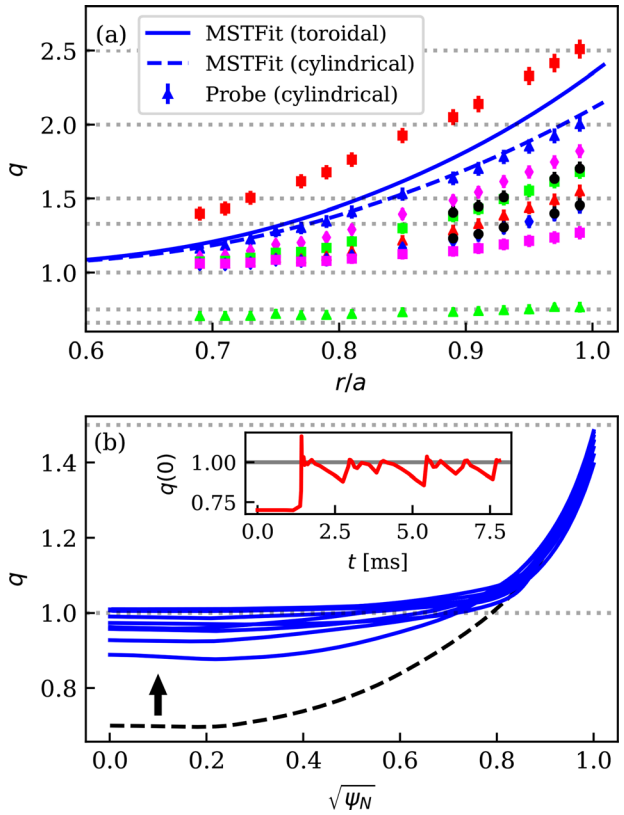

FIG. 2. (a) Probe data showing equilibrium safety factor profiles with maximum depth $r/a = 0.69$ [colored symbols indicate different values of $q(a)$, independent from Fig. 1] and $r/a = 0.89$ for two cases $q_c(a) = 1.55$ and 1.8 (black circles). A toroidal equilibrium reconstruction of q (solid) and q_c (dashed) is shown for $q_c(a) = 2.1$. Low-order rational values are indicated with dotted lines. (b) Safety factor profile and (inset) central value evolution from a NIMROD simulation with $q(a) = 1.5$, where profiles are shown spanning the minor radius at $t = 0$ (dashed black) and evenly spaced over $1.8 \leq t \leq 7.8$ ms (solid blue). The black arrow indicates raising of $q(0)$ during an initial transient period.

in the interior and become flatter as $q(a)$ decreases, consistent with evidence of current profile broadening shown in Fig. 1(c). This is indicative of a self-organization process in which the current distribution is rearranged due to mode activity such that the interior $q(r)$ remains near unity, even as the total current is varied. Thus, a mechanism similar to the sawtooth cycle in standard tokamaks also appears to be active in the range $1 < q(a) < 2$. Data are omitted for cases $q(a) \approx 1$ due to the presence of a strong, saturated 1/1 helical structure, the analysis of which is complicated and beyond the scope of this work. Data are shown with smaller probe depth $r/a = 0.89$ for $q_c(a) = 1.8$ and 1.55 to demonstrate that $q(r)$ is not altered by the probe at depth $r/a = 0.69$. Depths $r/a < 0.69$ were avoided due to observed probe-induced alterations of the $q(r)$ profile and dynamics.

An example MSTFit reconstruction of the $q(r)$ profile and its cylindrical approximation is also shown in Fig. 2(a). Although $q(0)$ is not directly measured, in Fig. 2(a) and the experimental data analysis to follow, an artificial constraint $q(0) = 1$ is implemented in MSTFit in order to best reflect the self-organization process thought to be active. This does not increase the error between the reconstruction and the probe data. Equilibrium reconstructions constrained by central measurements of the magnetic field in DIII-D also showed $q(0) \sim 1$ for transiently achieved $q_{95} \geq 1.87$.[26]

Nonlinear MHD simulations using the NIMROD code[44] are initialized using low-$q(a)$ toroidal equilibrium reconstructions calculated by MSTFit. Here, it is necessary to remove the $q(0) = 1$ constraint and initialize NIMROD with $q(0) < 1$ in order to excite the core 1/1 mode. Otherwise, sawtooth-like behavior is not observed. NIMROD solves the 3D extended, visco-resistive MHD equations using a finite-element method in the poloidal plane, a truncated Fourier representation in the toroidal direction, and a semi-implicit time-advance algorithm. An ideal-wall boundary condition at $r = a$ and Lundquist number of $S = 10^5$ are used to reproduce experimental conditions. Based on convergence tests for similar computations, the simulations conducted here use a poloidal mesh of 1620 bicubic elements, toroidal modes $n \leq 10$, and Prandtl number $Pr = 5$. They compute the nonlinear evolution of perturbations about the equilibrium profiles determined by MSTFit. They are sensitive to profile details but not to initial perturbations.

An example of the evolution of the $q(\sqrt{\psi_N})$ profile and central value $q(0)$ is shown in Fig. 2(b) for a simulation with $q(a) = 1.5$, where ψ_N is the normalized poloidal flux, representing the minor radial location in the plasma. The simulation features an early transient period where an $n = 1$ instability grows and drives q upward in the core, followed by cyclical sawtooth fluctuations. The initial profile from MSTFit is plotted as well as those during three sawtooth cycles, demonstrating that $q(0)$ is held between 0.85 and 1 due to the instability. Similar behavior is observed in separate NIMROD runs with $q(a) = 1.8$ and 2.5. Poincaré visualization of magnetic surfaces shows that these cases are roughly consistent with the Kadomtsev model of regular, periodic sawtooth reconnection,[2,4] although the results were found to be somewhat sensitive to the $q(r)$ profile used for initialization. Overall, these simulations support the experimental implication that $q(0) \sim 1$ for $1 < q(a) < 2$.

Experimental probe data indicate that the interior safety factor also remains near unity when $q(a) = 1$ is approached dynamically from above in a single discharge. This is illustrated in Fig. 3, where I_p is ramped upward from 50 to 90 kA starting at 25 ms. The safety factor at the edge decreases as $1/I_p$, whereas inside the plasma it stops decreasing near unity. Periodic sawtooth crashes are observed in the probe signals prior to, and early in the current ramp. Fluctuations on

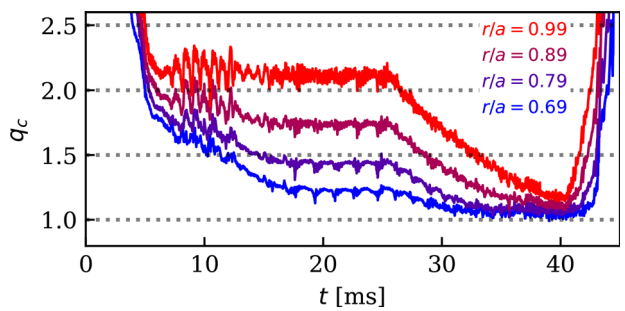

FIG. 3. Waveforms of cylindrical safety factor from the magnetic probe at four equidistant radial locations for a single discharge in which I_p is initially held steady and then ramped upward from 25 to 40 ms.

the probe channels nearest the wall are associated with 10 kHz switching of the PPS.

Probe measurements of magnetic fluctuations are presented in Fig. 4 for steady discharges over the range $1.7 \leq q(a) \leq 3$. For $q(a) = 3$, the signals show periodicity at 0.4 kHz associated with the sawtooth cycle, and faster oscillations associated with rotating modes during the crash. For $q(a) = 1.9$ and 1.7, the signals become irregular, and the power spectrum is broadened. Although these measurements are made locally, they are consistent with the change in behavior at lower $q(a)$ observed in global measurements such as Λ in Fig. 1(c). Data (not shown) from magnetic coil arrays mounted on the plasma-facing wall also exhibit this trend. Periodic bursts of activity with a dominant $n = 1$ component are measured at higher values of $q(a)$, gradually transitioning at lower $q(a)$ to irregularity with $1 \leq n \leq 3$ having similar amplitudes. The same behavior is observed in cases where the probe is withdrawn, implying that the change is not due to plasma–probe interaction.

The confinement properties of steady plasmas spanning $1.3 \leq q(a) \leq 3$ are shown in Fig. 5, with I_p ranging from 40 to 90 kA and the loop voltage, V_{loop}, ranging from 2 to 20 V. Core-averaged ($r/a < 0.2$) Thomson scattering measurements show the electron temperature generally decreasing for $q(a) < 2$, with a slight local maximum near 2. Similar to the behavior of $j_\phi(r)$ discussed above, the $T_e(r)$ and $n_e(r)$ profiles (not shown) become broader and flatter, implying rapid thermal transport, as $q(a)$ decreases. The Ohmic input power, $P_{\text{ohm}} = I_p V_{\text{loop}}$, increases dramatically at low $q(a)$. This is in agreement with the MSTFit calculation based on neoclassical resistivity, η, and spatially constant effective ionic charge, $Z_{\text{eff}} = 1.5$. This value of Z_{eff} was chosen such that the volume average of ηj computed by MSTFit matched the experimentally measured toroidal electric field. The normalized plasma beta, $\beta_N \equiv \beta a B / I_p[\text{MA}]$, is well below the empirical Troyon limit, $\beta_N = 2.8\%$,[9] as can be expected in a plasma without auxiliary heating. The electron energy confinement time, $\tau_{E,e}$, is calculated from MSTFit, constrained by measurements of T_e and the magnetic probe data at depths $r/a \geq 0.69$. Measurements of the ion temperature are not available, but we also show the total confinement time, τ_E, based on the assumptions $T_i/T_e = 1$ and $n_i/n_e = 0.8$. The widely used neo-Alcator confinement scaling $\tau_{\text{NA}} = 7 \times 10^{-22} \langle n_e \rangle q(a) R^2 a$[51,52] is shown for reference with a light blue band indicating the range in density. The measured confinement decreases at lower $q(a)$ faster than τ_{NA}, suggesting a qualitative difference in confinement physics relative to standard tokamak plasmas with $q(a) \gtrsim 2.5$ on which the scaling is based. The small increase in confinement for $q(a) \approx 2$ might be due to stabilization of the 2/1 mode by proximity to the conducting wall. Variation of confinement with density in MST tokamak plasmas has not yet been explored yet in detail. Confinement may be reduced for $q(a) = 3$ due to proximity to the Greenwald density limit.[10] We suspect that for $q(a) < 2$, the confinement is governed largely by MHD activity, as opposed to drift-wave turbulence which has been implicated in both linear and saturated Ohmic confinement.[52]

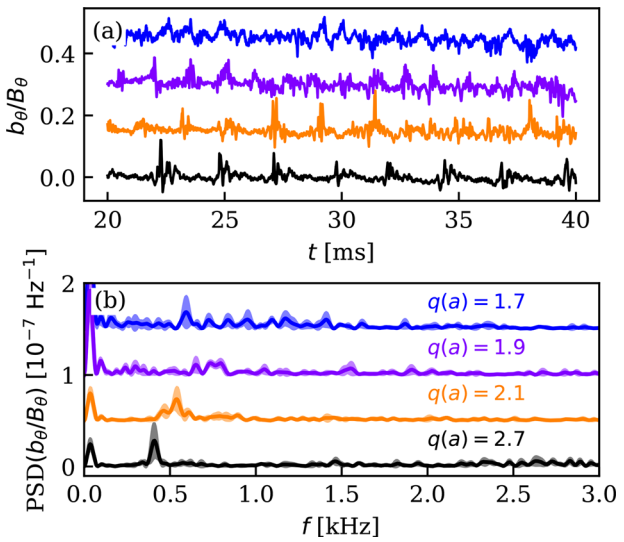

FIG. 4. (a) Probe measurements of normalized poloidal field fluctuations at $r/a = 0.89$, and (b) power spectral density averaged over three coils $0.89 \leq r/a \leq 0.93$ and three identical discharges. Values of $q(a)$ for both plots are indicated in (b). For clarity, vertical offsets of 0.1 and 0.5 are added between waveforms in (a) and (b), respectively.

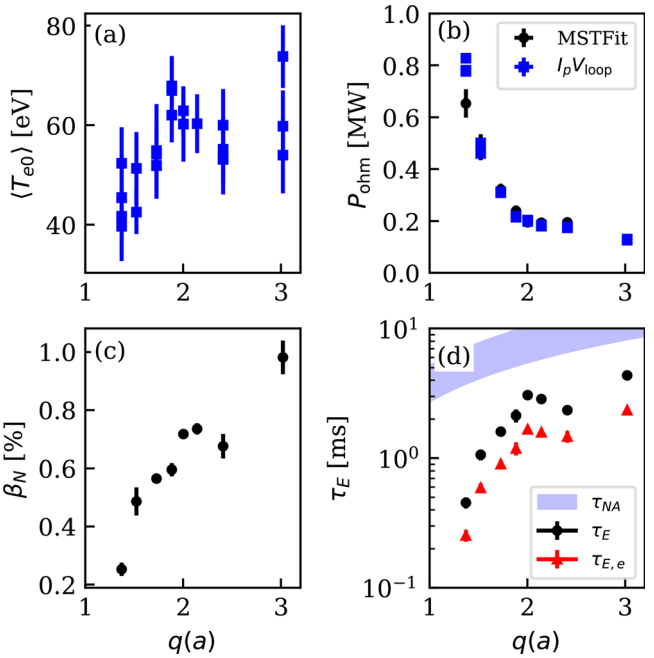

FIG. 5. Variation of plasma parameters with $q(a)$, including (a) core-averaged electron temperature, (b) Ohmic input power, (c) normalized plasma beta, and (d) total and electron energy confinement time calculated by MSTFit, where assumptions of ion properties are discussed in the text and the neo-Alcator scaling is shown.[51]

Multiple conclusions can be drawn from these results. First, self-organization of the toroidal current density profile persists in the range $1 < q(a) < 2$, holding $q(0) \approx 1$ across a core region with little or no magnetic shear which expands outward as $q(a)$ decreases. Second, the MHD activity changes character from discrete sawtooth crashes to irregular, quasi-continuous relaxation as $q(a)$ decreases. Finally, confinement decreases rapidly as $q(a)$ is lowered from 2 toward 1. The transition to irregular MHD behavior could be associated with pressure-driven modes which are unstable in the absence of shear[53]

and/or interaction of the internal 1/1 kink instability with the conducting wall. It suggests that the magnetic topology may become largely stochastic as $q(a)$ decreases below 2, which is consistent with the observation of broad, flat T_e and n_e profiles and decreased confinement. Further work is needed to understand why the irregular behavior at low $q(a)$ was not found consistently in the numerical modeling with NIMROD, including a more comprehensive study of sensitivity to the initial equilibrium. Future experimental work at higher S will help clarify the influence of resistive effects on this change in behavior.

These results suggest that operation near or slightly below $q(a) = 2$ could be useful for tokamak fusion devices if the external 2/1 mode can be stabilized. In this scenario, the modest decrease in confinement shown here is balanced against the benefits of higher plasma current and removal of the $q = 2$ surface from the plasma interior. Additionally, deeper understanding of fluctuations and transport in this regime may uncover possibilities for optimization and/or improved confinement. Importantly, this work further demonstrates that current-driven tokamak disruptions may be circumvented through the combination of passive stabilization due to a nearby conducting wall and advanced feedback power supplies capable of sustaining plasma current in highly resistive conditions. Finally, this work opens the possibility of studying steady, long-lived toroidal plasmas in a regime between the RFP and tokamak which was not possible previously.

This material is based upon the work supported by the U.S. Department of Energy (DOE) Office of Science, Office of Fusion Energy Sciences program under Award No. DE-SC0020245. The experiments were conducted at the Wisconsin Plasma Physics Laboratory (WiPPL), a research facility supported by the DOE Office of Fusion Energy Sciences under contract DE-SC0018266 with major facility instrumentation developed with support from the National Science Foundation under award PHY 0923258. The numerical simulations were performed using the computer resources and assistance of the UW-Madison Center For High Throughput Computing (CHTC) in the Department of Computer Sciences. The CHTC is supported by UW-Madison, the Advanced Computing Initiative, the Wisconsin Alumni Research Foundation, the Wisconsin Institutes for Discovery, and the National Science Foundation, and is an active member of the OSG Consortium, which is supported by the National Science Foundation and the U.S. Department of Energy's Office of Science.

AUTHOR DECLARATIONS

Conflict of Interest

The authors have no conflicts to disclose.

Author Contributions

N. C. Hurst: Conceptualization (lead); Formal analysis (lead); Investigation (lead); Methodology (equal); Software (equal); Visualization (lead); Writing – original draft (lead). **D. J. Den Hartog:** Investigation (equal); Methodology (equal); Resources (equal); Writing – review and editing (equal). **C. B. Forest:** Funding acquisition (equal); Project administration (equal); Supervision (equal); Validation (equal); Writing – review and editing (equal). **M. D. Pandya:** Formal analysis (equal); Methodology (equal); Resources (equal); Writing – review and editing (equal). **W. S. Solsrud:** Methodology (equal); Software (equal). **B. E. Chapman:** Conceptualization (equal); Funding acquisition (lead); Project administration (lead); Supervision (lead); Writing – review and editing (equal). **A. F. Almagri:** Methodology (equal); Resources (equal); Writing – review and editing (supporting). **B. S. Cornille:** Investigation (equal); Methodology (equal); Software (equal); Visualization (equal). **S. Z. Kubala:** Investigation (equal); Methodology (equal); Resources (equal). **K. J. McCollam:** Methodology (equal); Validation (equal); Writing – review and editing (equal). **J. S. Sarff:** Formal analysis (equal); Resources (equal); Supervision (equal); Validation (equal); Writing – review and editing (equal). **C. R. Sovinec:** Investigation (equal); Software (equal); Supervision (equal); Writing – review and editing (equal). **J. K. Anderson:** Methodology (equal); Resources (equal); Software (equal).

DATA AVAILABILITY

The data that support the findings of this study are available from the corresponding author upon reasonable request.

REFERENCES

[1]A. Hasegawa, Adv. Phys. **34**, 1–42 (1985).
[2]B. B. Kadomtsev, Sov. J. Plasma Phys. **1**, 389 (1976).
[3]R. J. Hastie, Astrophys. Space Sci. **256**, 177 (1997).
[4]J. Wesson, *Tokamaks*, 3rd ed. (Oxford University Press, Oxford, UK, 2004).
[5]S. C. Jardin, I. Krebs, and N. Ferraro, Phys. Plasmas **27**, 032509 (2020).
[6]W. W. Heidbrink and B. S. Victor, Phys. Plasmas **27**, 080701 (2020).
[7]D. Biskamp, *Nonlinear Magnetohydrodynamics* (Cambridge University Press, Cambridge, UK, 1993).
[8]P. C. de Vries, M. F. Johnson, B. Alper, P. Buratti, T. C. Hender, H. R. Koslowski, V. Riccardo, and J.-E. Contributors, Nucl. Fusion **51**, 053018 (2011).
[9]J. Friedberg, *Plasma Physics and Fusion Energy* (Cambridge University Press, New York, 2007).
[10]M. Greenwald, Plasma Phys. Controlled Fusion **44**, R27 (2002).
[11]L. Marrelli, P. Martin, M. E. Puiatti, J. S. Sarff, B. E. Chapman, J. R. Drake, D. F. Escande, and S. Masamune, Nucl. Fusion **61**, 023001 (2021).
[12]T. R. Jarboe, Plasma Phys. Controlled Fusion **36**, 945 (1994).
[13]J. B. Taylor, Rev. Mod. Phys. **58**, 741 (1986).
[14]U. Shumlak, B. A. Nelson, R. P. Golingo, S. L. Jackson, E. A. Crawford, and D. J. D. Hartog, Phys. Plasmas **10**, 1683 (2003).
[15]V. V. Ivanov, J. P. Chittenden, S. D. Altemara, N. Niasse, P. Hakel, R. C. Mancini, D. Papp, and A. A. Anderson, Phys. Rev. Lett. **107**, 165002 (2011).
[16]D. M. Rust and A. Kumar, Astrophys. J. **464**, L199 (1996).
[17]A. Hassanin and B. Kliem, Astrophys. J. **832**, 106 (2016).
[18]P. Wongwaitayakornkul, H. Li, and P. M. Bellan, Astrophys. J. **895**, L7 (2020).
[19]E. E. Lawrence and W. Gekelman, Phys. Rev. Lett. **103**, 105002 (2009).
[20]C. Paz-Soldan, M. I. Brookhart, A. J. Clinch, D. A. Hannum, and C. B. Forest, Phys. Plasmas **18**, 052114 (2011).
[21]P. Shi, P. Srivastav, C. Beatty, R. John, M. Lazo, J. McKee, J. McLaughlin, M. Moran, M. Paul, E. E. Scime, E. E. Scime, D. Thompson, and T. Steinberger, Phys. Plasmas **28**, 032101 (2021).
[22]M. W. Scheeler, W. M. V. Rees, H. Kedia, D. Kleckner, and W. T. M. Irvine, Science **357**, 487 (2017).
[23]J. M. Finn, Phys. Plasmas **2**, 198 (1995).
[24]M. Baruzzo, T. Bolzonella, Y. Q. Liu, G. Manduchi, G. Marchiori, A. Soppelsa, M. Takechi, and F. Villone, Nucl. Fusion **52**, 103001 (2012).
[25]P. Piovesan, J. M. Hanson, P. Martin, G. A. Navratil, F. Turco, J. Bialek, N. M. Ferraro, R. J. L. Haye, M. J. Lanctot, M. Okabayashi, C. Paz-Soldan, E. J. Strait, A. D. Turnbull, P. Zanca, M. Baruzzo, T. Bolzonella, A. W. Hyatt, G. L. Jackson, L. Marrelli, L. Piron, and D. Shiraki, Phys. Rev. Lett. **113**, 045003 (2014).
[26]J. M. Hanson, J. M. Bialek, M. Baruzzo, T. Bolzonella, A. W. Hyatt, G. L. Jackson, J. King, R. J. L. Haye, M. J. Lanctot, L. Marrelli, P. Martin, G. A.

Navratil, M. Okabayashi, K. E. J. Olofsson, C. Paz-Soldan, P. Piovesan, C. Piron, L. Piron, D. Shiraki, E. J. Strait, D. Terranova, F. Turco, A. D. Turnbull, and P. Zanca, Phys. Plasmas **21**, 072107 (2014).
[27]P. Brunsell, J. R. Drake, S. Mazur, and P. Nordlund, Phys. Scr. **44**, 358 (1991).
[28]P. L. Taylor, R. J. LaHaye, M. J. Schaffer, T. Tamano, N. Inoue, Z. Yoshida, and Y. Kamada, Nucl. Fusion **29**, 92 (1989).
[29]Y. Kamada, T. Fujita, Y. Murakami, T. Ohira, K. Saitoh, Y. Fuke, M. Utsumi, Z. Yoshida, and N. Inoue, Nucl. Fusion **29**, 713 (1989).
[30]Z. Yoshida, N. Inoue, T. Fujita, K. Hattori, S. Ishida, K. Itami, Y. Kamada, S. Kido, J. Morikawa, H. Morimoto, Y. Murakami, H. Nakanishi, Y. Ogawa, K. Saitoh, S. Takeji, M. Watanabe, and H. Yamada, J. Plasma Phys. **59**, 103 (1998).
[31]P. K. Chattopadhyay, R. Pal, A. N. S. Iyengar, and J. Ghosh, Phys. Rev. Lett. **81**, 3151 (1998).
[32]D. Group, Nucl. Fusion **20**, 271 (1980).
[33]S. Lahiri, A. N. S. Iyengar, S. Mukhopadhyay, and R. Pal, Nucl. Fusion **36**, 254 (1996).
[34]T. Group, Nucl. Fusion **24**, 784 (1984).
[35]H. Y. W. Tsui, R. J. LaHaye, and J. A. Cunnane, Nucl. Fusion **30**, 59 (1990).
[36]M. Zuin, M. Agostini, F. Auriemma, D. Bonfiglio, S. Cappello, L. Carraro, R. Cavazzana, L. Cordaro, P. Franz, L. Marrelli, E. Martines, M. E. Puiatti, R. Piovan, G. Spizzo, D. Terranova, N. Vianello, P. Zanca, B. Zaniol, and L. Zanotto, Nucl. Fusion **62**, 066029 (2022).
[37]M. D. Pandya, M. C. ArchMiller, M. R. Cianciosa, D. A. Ennis, J. D. Hanson, G. J. Hartwell, J. D. Hebert, J. L. Herfindal, S. F. Knowlton, X. Ma, S. Massidda, D. A. Maurer, N. A. Roberds, and P. J. Traverso, Phys. Plasmas **22**, 110702 (2015).
[38]K. Kusano, T. Sato, H. Yamada, Y. Murakami, Z. Yoshida, and N. Inoue, Nucl. Fusion **28**, 89 (1988).
[39]K. Suzuki, Z. Yoshida, and K. Kusano, Nucl. Fusion **31**, 179 (1991).
[40]D. Bonfiglio, S. Cappello, R. Piovan, L. Zanotto, and M. Zuin, Nucl. Fusion **48**, 115010 (2008).
[41]R. N. Dexter, D. W. Kerst, T. W. Lovell, S. C. Prager, and J. C. Sprott, Fusion Tech. **19**, 131 (1991).
[42]D. J. Holly, J. R. Adney, K. J. McCollam, J. C. Morin, and M. A. Thomas, in *IEEE/NPSS 24th Symposium on Fusion Engineering* (IEEE, 2011).
[43]I. R. Goumiri, K. J. McCollam, A. A. Squitieri, D. J. Holly, J. S. Sarff, and S. P. Leblanc, Plasma Res. Express **2**, 035012 (2020).
[44]C. R. Sovinec, T. A. Gianakon, E. D. Held, S. E. Kruger, D. D. Schnack, and NIMROD Team, Phys. Plasmas **10**, 1727 (2003).
[45]J. S. Sarff, A. F. Almagri, J. K. Anderson, M. Borchardt, W. Cappechi, D. Carmody, K. Caspary, B. E. Chapman, D. J. D. Hartog, J. Duff, S. Eilerman, A. Falkowski, C. B. Forest, M. Galante, J. A. Goetz, D. J. Holly, J. Koliner, S. Kumar, J. D. Lee, D. Liu, K. J. McCollam, M. McGarry, V. V. Mirnov, L. Morton, S. Munaretto, M. D. Nornberg, P. D. Nonn, S. P. Oliva, E. Parke, M. J. Pueschel, J. A. Reusch, J. Sauppe, A. Seltzman, C. R. Sovinec, D. Stone, D. Theucks, M. Thomas, J. Triana, P. W. Terry, J. Waksman, G. C. Whelan, D. L. Brower, W. X. Ding, L. Lin, D. R. Demers, P. Fimognari, J. Titus, F. Auriemma, S. Cappello, P. Franz, P. Innocente, R. Lorenzini, E. Martines, B. Momo, P. Piovesan, M. Puiatti, M. Spolaore, D. Terranova, P. Zanca, V. I. Davydenko, P. Deichuli, A. A. Ivanov, S. Polosatkin, N. V. Stupishin, D. Spong, D. Craig, H. Stephens, R. W. Harvey, M. Cianciosa, J. D. Hanson, B. N. Breizman, M. Li, and L. J. Zheng, Nucl. Fusion **55**, 104006 (2015).
[46]S. Munaretto, B. E. Chapman, B. S. Cornille, A. M. Dubois, K. J. McCollam, C. R. Sovinec, A. F. Almagri, and J. A. Goetz, Nucl. Fusion **60**, 046024 (2020).
[47]I. H. Hutchinson, *Principles of Plasma Diagnostics*, 2nd ed. (Cambridge University Press, New York, 2002).
[48]S. Z. Kubala, M. T. Borchardt, D. J. D. Hartog, D. J. Holly, C. M. Jacobson, L. A. Morton, and W. C. Young, Rev. Sci. Instrum. **87**, 11E547 (2016).
[49]E. Parke, W. X. Ding, J. Duff, and D. L. Brower, Rev. Sci. Instrum. **87**, 11E115 (2016).
[50]J. K. Anderson, C. B. Forest, T. M. Biewer, J. S. Sarff, and J. C. Wright, Nucl. Fusion **44**, 162 (2004).
[51]R. J. Goldston, Plasma Phys. Controlled Fusion **26**, 87 (1984).
[52]J. E. Rice, J. Citrin, N. M. Cao, P. H. Diamond, M. Greenwald, and B. A. Grierson, Nucl. Fusion **60**, 105001 (2020).
[53]J. A. Wesson, Plasma Phys. Controlled Fusion **28**, 243 (1986).